INT. J. NUM. METH. HEAT FLUID FLOW, VOL. 6, 63–76 (1996)

THE APPLICATION OF SPLIT-COEFFICIENT MATRIX METHOD TO TRANSIENT TWO PHASE FLOWS

D. M. LU†, H. C. SIMPSON‡ AND A. GILCHRIST‡

†*Faculty of Mechanical Engineering, Technion, Haifa 32000, Israel.* ‡*Division of Energy Systems Studies, Department of Mechanical Engineering, University of Strathclyde, UK*

ABSTRACT

An easy-to-use numerical model for transient two-phase pipe flow analyses was developed by applying the split-coefficient matrix method (SCMM) to a homogeneous equilibrium two-phase flow model. The basic idea of the SCMM is to split the Jacobian coefficient matrix into two sub-vectors, each associated with eigenvalues of the same sign. Hence, one-sided finite difference schemes can accordingly be applied to the sub-vectors. The present model was validated against experiments. It is numerically stable provided that a criterion is met due to the use of a time explicit format. The satisfactory agreement between the numerical and experimental results indicates that the model may be used as a simple, efficient tool for general engineering analyses of transient two-phase flow. The advantages of applying SCMM to transient two phase flows are briefly addressed, and it is applicable to systems having real eigenvalues.

KEY WORDS Two phase flow Split-coefficient matrix

INTRODUCTION

Transient two-phase flow has significant application in many important engineering systems, e.g. nuclear reactors, heat exchangers, material processing and de-aerator systems. Although it has been under extensive investigations for the last two decades and substantial progress has been made in modelling transient two-phase flows, the prediction of transient two-phase flow remains a challenging task due to the extreme complexity of the flow arisen from the phasic interactions and also due to our limited ability to handle the problem.

The present work was motivated by the simulation studies of the pressure decay transient of a de-aerator system, where it is essential to be able to appropriately estimate the transient behaviours of downcomer two-phase flow, in particular, the variation of downcomer pressure in order to effectively protect the Boiler Feed Pump (BFP), situated right after the downcomer, from cavitation.

Considering its engineering background, the prime objective of the present work was to develop a simple reliable numerical model which may easily be coded and used by engineers, who may not be CFD experts, for transient two-phase flow analyses.

MATHEMATICAL MODEL AND NUMERICAL METHOD

Although a number of two-phase flow models (Wallis[1], Ishii[2], and Banerjee and Hancox[3] may be referred to for a comprehensive account of two-phase flow modelling) have been proposed over the past years, it is recognized that none of them have general applicability. Two-phase flow models are flow regime dependent owing to a lack of knowledge about the general picture of the complex interfacial transport phenomena.

0961–5539/96/030063–14$2.00

Received August 1994
Revised January 1995

Amongst the available two-phase flow models, from the simplest homogeneous equilibrium model (HEM) to the more complicated two-fluid models, HEM is widely used for general analyses due to its simplicity and convenience. It has been successfully applied to certain flow regimes such as dispersed flows or even sometimes transitional flows. Although there are cases where HEM does not properly model what really happens, nevertheless, it can be used to give a primary estimate. Another advantage of HEM is that its mathematical representation is always a well-posed initial-boundary value problem, namely its system of governing equations is hyperbolic while most two-phase flow models, in particular, those used in the complicated system codes, are ill-posed systems due to the improper forms accounting for the phasic interactions and thus have complex eigenvalues which make these models vulnerable to numerical instability. For ill-posed systems, specific numerical techniques, e.g. artificial damping terms, staggered mesh and donor-cell techniques are used to make the numerical schemes stable at the cost of loss of accuracy due to the considerable numerical diffusion introduced by these measures and also at the cost of increased complexity of the numerical models. Work of this kind may be referred to Micaelli[4] and Jackson *et al.*[5], and there has been little change from the algorithms of the first field codes.

In the light of the above points and the objective of the present work, HEM was chosen to describe downcomer transient two-phase flows. It also provided a good foundation for testing the numerical technique to be used to solve the equations governing the flow, which was expected to yield a stable numerical model convenient for coding. Of course, more complicated physical considerations may be taken into account in the modelling work if it is desirable or of interest.

The mathematical model

For one dimensional (1-D), adiabatic, homogeneous, equilibrium transient two-phase flow illustrated as in *Figure 1*, the conservation equations are written as follows,

Mass equation
$$\frac{\partial \alpha}{\partial t}+\frac{(\rho k)_m}{\rho_{gf}}\frac{\partial P}{\partial t}+\frac{\partial G}{\partial z}\frac{1}{\rho_{gf}}=0 \tag{1}$$

Momentum equation
$$\frac{\partial G}{\partial t}+\frac{2G}{\rho_m}\frac{\partial G}{\partial z}+\left[1-\frac{G^2}{\rho_m^2}(\rho k)_m\right]\frac{\partial P}{\partial z}-\frac{G^2\rho_{gf}}{\rho_m^2}\frac{\partial \alpha}{\partial z}=a \tag{2}$$

Energy equation
$$\frac{\partial P}{\partial t}+\frac{G}{\rho_m}\frac{\partial P}{\partial z}+\frac{\rho_f\rho_g h_{gf}}{\rho_m d}\left(\frac{\partial \alpha}{\partial t}+\frac{G}{\rho_m}\frac{\partial \alpha}{\partial z}\right)=\frac{b}{d} \tag{3}$$

Equation (3) is derived by assuming that the vapour phase can be approximated as a perfect gas and by neglecting the coefficient of volume expansion of the liquid.

In the above equations α is the void fraction, P is the static pressure, G is the mass velocity of the homogeneous fluid, and ρ_m is defined as,

$$\rho_m=\alpha\rho_g+(1-\alpha)\rho_f \tag{4}$$

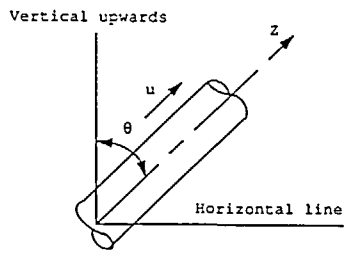

Figure 1 Schematic of one-dimensional homogeneous equilibrium flow

where ρ_g and ρ_f are the saturation densities of vapour and liquid, respectively.

$$(\rho k)_m=\alpha\rho_g k_g+(1-\alpha)\rho_f k_f \tag{5}$$

$$k_i=\frac{1}{\rho_i}\frac{\partial\rho_i}{\partial P}, \qquad i=g, f \tag{6}$$

$$\rho_{gf}=\rho_g-\rho_f \tag{7}$$

$$a=-\rho_m g\cos\theta-F_w \tag{8}$$

$$b=\frac{G}{\rho_m}F_w \tag{9}$$

for downcomer flows, $\theta=\pi$, F_w is the viscous friction which can be expressed by,

$$F_w=sign(G)\frac{4f_n G^2}{2D_d\rho_m} \tag{10}$$

where f_n is Fanning coefficient, D_d is the diameter of downcomer tube; $sign(G)$ is positive sign when G is forwards and negative sign when G is backwards.

$$d=\beta(\rho C_p)_m+\alpha(1-\alpha)\rho_f\rho_g h_{gf}k_{gf}/\rho_m-\alpha \tag{11}$$

$$\beta=\left(\frac{\mathrm{d}T}{\mathrm{d}P}\right)_s=\frac{T}{h_{gf}}(v_g-v_f) \tag{12}$$

where h_{gf} is the fluid enthalpy of evaporation, v_g and v_f are the specific volumes of vapour and liquid phases, respectively, and subscript s denotes saturation.

$$(\rho C_p)_m=\alpha\rho_g C_{pg}+(1-\alpha)\rho_f C_{pf} \tag{13}$$

$$k_{gf}=k_g-k_f \tag{14}$$

where C_{pg} and C_{pf} are the specific heat of vapour and liquid at constant pressure, respectively.

After certain operations, (1), (2) and (3) can be transformed into the following equivalent matrix form,

$$\frac{\partial W}{\partial t}+\boldsymbol{D}\frac{\partial W}{\partial z}=\boldsymbol{E} \tag{15}$$

where

$$W=[G\ P\ \alpha]^T \tag{16}$$

$$\boldsymbol{D}=\begin{bmatrix} 2\dfrac{G}{\rho_m} & 1-\dfrac{G^2}{\rho_m^2}(\rho k)_m & -\dfrac{G^2\rho_{gf}}{\rho_m^2} \\ -\dfrac{\rho_f\rho_g h_{gf}}{\rho_{gf}\rho_m de} & \dfrac{G}{\rho_m e} & \dfrac{G}{\rho_m}\dfrac{\rho_f\rho_g h_{gf}}{\rho_m de} \\ \dfrac{1}{\rho_{gf}e} & -\dfrac{G}{\rho_m}\dfrac{(\rho k)_m}{\rho_{gf}e} & -\dfrac{G}{\rho_m}\dfrac{\rho_f\rho_g h_{gf}}{\rho_m d}\dfrac{(\rho k)_m}{\rho_{gf}e} \end{bmatrix} \tag{17}$$

$$\boldsymbol{E}=\begin{bmatrix} a & \dfrac{b}{de} & -\dfrac{b(\rho k)_m}{d\rho_{gf}e} \end{bmatrix}^T \tag{18}$$

$$e=1-\frac{\rho_f\rho_g h_{gf}}{\rho_m d}\frac{(\rho k)_m}{\rho_{gf}} \tag{19}$$

Numerical method—split-coefficient matrix method (SCMM)

Equation system (15) is a well-posed hyperbolic problem, it has three real eigenvalues which can be expressed as,

$$\lambda_1 = \frac{G}{\rho_m} + C \tag{20}$$

$$\lambda_2 = \frac{G}{\rho_m} - C \tag{21}$$

$$\lambda_3 = \frac{G}{\rho_m} \tag{22}$$

where C is the sonic velocity expressed as,

$$C = \sqrt{-\frac{\rho_f \rho_g h_{gf}}{\rho_m \rho_{gf} de}} \tag{23}$$

An analytical solution to equation system (15) is not known for general cases but numerical methods have to be used to obtain solutions. Apart from the numerical techniques mentioned previously, which also have applications in well-posed two-phase flow problems in combination with finite difference or finite volume method, the method of characteristics (MOC), introduced by Courant *et al.*[6], is often used in two-phase flow field to solve hyperbolic partial differential equation (PDS) systems, e.g. Hancox *et al.*[7] and Ng[8]. The advantage of MOC is that it considers the propagation of certain signals or disturbances along the characteristic lines, then a one-sided finite difference scheme can be applied according to the direction of the propagation, and hence ensures the numerical stability of the scheme due to its consistency with physics. MOC is believed to be of higher resolution than the methods mentioned previously as it does not introduce the kind of numerical diffusion the above methods have. However, the characteristic lines have to be determined, with reference to a time-space frame or time-space meshes, as well as solving the PDEs along these lines, both numerically. The efforts of determining the characteristic lines may not be daunting for one dimensional transient flows, they certainly become cumbersome when two or three dimensional initial value problems are of concern or more complicated two-phase flow models such as two-fluid models are used. This practically prohibits the application of MOC to such complicated problems.

A method referred to as split-coeffiicient matrix method (SCMM) has been used to solve single phase flow PDEs in gas- and aerodynamic fields (see Chakravarthy *et al.*[9], Steger[10], and Steger and Warming[11]). This method has more advantages over MOC in that it not only ensures the numerical stability by making use of the direction of signal propagation and has higher resolution like MOC owing to the reasons mentioned above, but it is much easier to use, as far as programming is concerned, since it does not need characteristic lines to be constructed. This is achieved by doing some specific mathematical manipulations, which make use of the signal propagation. In these regards, we would think that SCMM has potential for transient two-phase flow studies. Its numerical convenience will become more prominent when 2-D or 3-D transient problems and two-fluid models are of interest although we are only dealing with 1-D transient two-phase flow here.

The basic idea of SCMM is to split the Jacobian matrix D of equations (15) or the flux vector into two sub-vectors, each in association with eigenvalues of the same sign (positive or negative). Thus one-sided backward and forward first order finite difference schemes can be applied according to the sign associated with each sub-vector. The derivation of sub-vectors from the original flux vector is purely mathematical operation. There is no numerical calculation involved at this stage. And the sub-vectors can be expressed as the algebraical functions of the major flow parameters. Hence it can be seen that SCMM is numerically more convenient than MOC

while in the mean time it reserves all the advantages MOC has, i.e. numerical stability and higher numerical resolution. This method was adopted in the present work to solve the downcomer transient two phase flow equation system. The use of SCMM for transient two phase flow calculation had not been seen in the open literature. Compared with single phase aero-dynamic flows, two-phase flow systems are more complicated due to the complex phasic interactions at the interfaces.

The eigen-vector matrix corresponding to λ_1, λ_2 and λ_3 is derived as,

$$T=\begin{bmatrix} 1 & \dfrac{1-\dfrac{G}{\rho_m}(\rho k)_m C}{C} & -\rho_{gf}\dfrac{G}{\rho_m} \\ 1 & \dfrac{1+\dfrac{G}{\rho_m}(\rho k)_m C}{-C} & -\rho_{gf}\dfrac{G}{\rho_m} \\ 0 & -\dfrac{1}{C^2 e} & \rho_{gf} \end{bmatrix} \tag{24}$$

Its inverse matrix is,

$$T^{-1}=\begin{bmatrix} \dfrac{1+\dfrac{G}{\rho_m C}}{2} & \dfrac{1-\dfrac{G}{\rho_m C}}{2} & \dfrac{G}{\rho_m} \\ \dfrac{C}{2} & -\dfrac{C}{2} & 0 \\ \dfrac{1}{2C\rho_{gf}e} & -\dfrac{1}{2C\rho_{gf}e} & \dfrac{1}{\rho_{gf}} \end{bmatrix} \tag{25}$$

where T and T^{-1} satisfy,

$$DT^{-1}\Lambda T \tag{26}$$

and Λ is the eigen value matrix written as,

$$\Lambda=\begin{bmatrix} \lambda_1 & 0 & 0 \\ 0 & \lambda_2 & 0 \\ 0 & 0 & \lambda_3 \end{bmatrix} \tag{27}$$

if we define,

$$\lambda_1^+=\frac{\lambda_1+|\lambda_1|}{2} \tag{28}$$

$$\lambda_2^+=\frac{\lambda_2+|\lambda_2|}{2} \tag{29}$$

$$\lambda_3^+=\frac{\lambda_3+|\lambda_3|}{2} \tag{30}$$

$$\lambda_1^-=\frac{\lambda_1-|\lambda_1|}{2} \tag{31}$$

$$\lambda_2^- = \frac{\lambda_2 - |\lambda_2|}{2} \tag{32}$$

$$\lambda_3^- = \frac{\lambda_3 - |\lambda_3|}{2} \tag{33}$$

it is clear that $(\lambda_1^+, \lambda_2^+, \lambda_3^+) \geqslant 0$, and $(\lambda_1^-, \lambda_2^-, \lambda_3^-) \leqslant 0$ no matter whether λ_1, λ_2 and λ_3 are positive or negative. It is also clear that,

$$\lambda_1 = \lambda_1^+ + \lambda_1^- \tag{34}$$

$$\lambda_2 = \lambda_2^+ + \lambda_2^- \tag{35}$$

$$\lambda_3 = \lambda_3^+ + \lambda_3^- \tag{36}$$

Thus (27) can be rearranged as,

$$\Lambda = \begin{bmatrix} \lambda_1^+ & 0 & 0 \\ 0 & \lambda_2^+ & 0 \\ 0 & 0 & \lambda_3^+ \end{bmatrix} + \begin{bmatrix} \lambda_1^- & 0 & 0 \\ 0 & \lambda_2^- & 0 \\ 0 & 0 & \lambda_3^- \end{bmatrix} = \Lambda^+ + \Lambda^- \tag{37}$$

Substituting (37) into (26) yields,

$$D = T^{-1}\Lambda^+ T + T^{-1}\Lambda^- T = D^+ + D^- \tag{38}$$

The details of D^+ and D^- are given in APPENDIX 1.

Having D^+ and D^-, (15) can be rewritten as,

$$\frac{\partial W}{\partial t} + D^+ \frac{\partial W}{\partial z} + D^- \frac{\partial W}{\partial z} = E \tag{39}$$

In (39), $D^+(\partial W/\partial Z)$ is the sub-vector flux corresponding to the eigenvalues with positive sign, thus a backward finite difference scheme can be applied to $D^+(\partial W/\partial Z)$. Similarly, a forward finite difference format is used for $D^-(\partial W/\partial Z)$ as it associates with the eigen values of negative sign. Hence an explicit finite difference equation of (15) is derived as follows,

$$W_j^{i+1} = W_j^i + E_j^i \Delta t - [D_j^{+i}(W_j^i - W_{j-1}^i) + D_j^{-i}(W_{j+1}^i - W_j^i)] \frac{\Delta t}{\Delta z} \tag{40}$$

Figure 2 illustrates the t-z mesh for the numerical solution of (40). It also indicates that two boundary conditions should be imposed at the top of the downcomer and one boundary condition be imposed at the bottom.

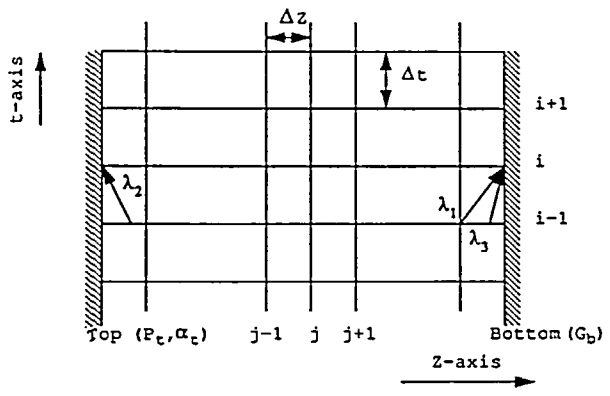

Figure 2 The t–z difference mesh for applying SCMM and the boundary conditions

VALIDATION OF THE NUMERICAL MODEL

The numerical model was validated against Ng's[8] and Lu's[12] experimental data.

Ng's experimental set-up comprised mainly a pressure drum, a downcomer tube, a circulating pump, a heater line and a heater by-pass line. R113, used as the working fluid, was circulated around the loop. An electrical heating unit was used to heat the fluid as it passed through the heater line between the pump outlet and the drum. Thus the initial pressure in the drum could be controlled for a particular run. The heater by-pass line was used to enable the isolation of the heater section just prior to conducting a test. The pump, which was a variable speed centrifugal pump, operated at various constant speeds dependent on the desired fluid velocity in the downcomer.

Lu's experimental apparatus was similar to Ng's but of different size and having different mechanism of causing depressurisation transient, and water was used as the working fluid.

In both experimental investigations, the systems initially ran under steady state, or equilibrium conditions. The depressurisation transients were triggered either by venting the contents in the drum (Ng's case) or by injecting cold water spray into the drum (Lu's case).

The serial numbers of their test runs represent various initial conditions and run set-ups, which, for Ng's tests, included the initial drum pressure P_{d0}, the initial volume of liquid in the drum V_0, the opening of the venting valve and the initial speed of the pump or the initial mass flow rate at the bottom of the downcomer $\dot{M}_{b0}$; while for Lu's tests, which included similar parameters but replacing the opening of the venting valve with the flow rate of the water spray $\dot{m}_{inj}$. The initial conditions for the calculations were obtained from the experimental initial values.

Some typical calculation results are presented below.

Numerical simulations of Ng's[8] experimental results of downcomer transient two-phase flow

As it is mentioned previously, for the numerical solution of downcomer transient two phase flow, it is necessary to impose two boundary conditions at the top and one at the bottom section of the downcomer.

In Ng's[8] experiments, such parameters as P_t and α_t at the top section, α_{mid} at the middle section and P_b and G_b at the bottom of the downcomer were measured. Hence Ng's experiments provide good information for exercising the numerical model; thus, the measured values of P_t, α_t and G_b were imposed at the top and the bottom sections as boundary conditions, respectively; and the measured α_{mid} and P_b were then compared with the results calculated from the present numerical model.

Although SCMM assures numerical stability, this statement is true in the present work only when the following condition is satisfied,

$$Co = \frac{|\lambda_{max}| \Delta t}{\Delta z} < 1 \tag{41}$$

Criterion (41) has to be met due to the use of the time explixit format of the finite difference scheme. The calculations were performed with a 50 node spatial mesh. The convergence tests showed that the model was stable provided that (41) was observed. However, it was found that an optimum Co was about 0.2 when the accuracy and the time step were both assessed. This relative small value of Co may reflect the inherent complexity of transient two-phase flows and may also be owing to the imposed boundary conditions which perhaps carry non-equilibrium flow information.

Applying this optimum Co, many Ng's tests were simulated. The typical CPU time is about 5 seconds for real transient time 10 sec on a Vax machine.

Figure 3 shows the typical boundary conditions. *Figure 4*, *Figure 5*, *Figure 6* and *Figure 7* present the predicted results of the bottom pressure P_b and the middle section void fraction α_{mid} in comparison with Ng's corresponding experimental results. The run set-ups of these tests may be found in Ng[8].

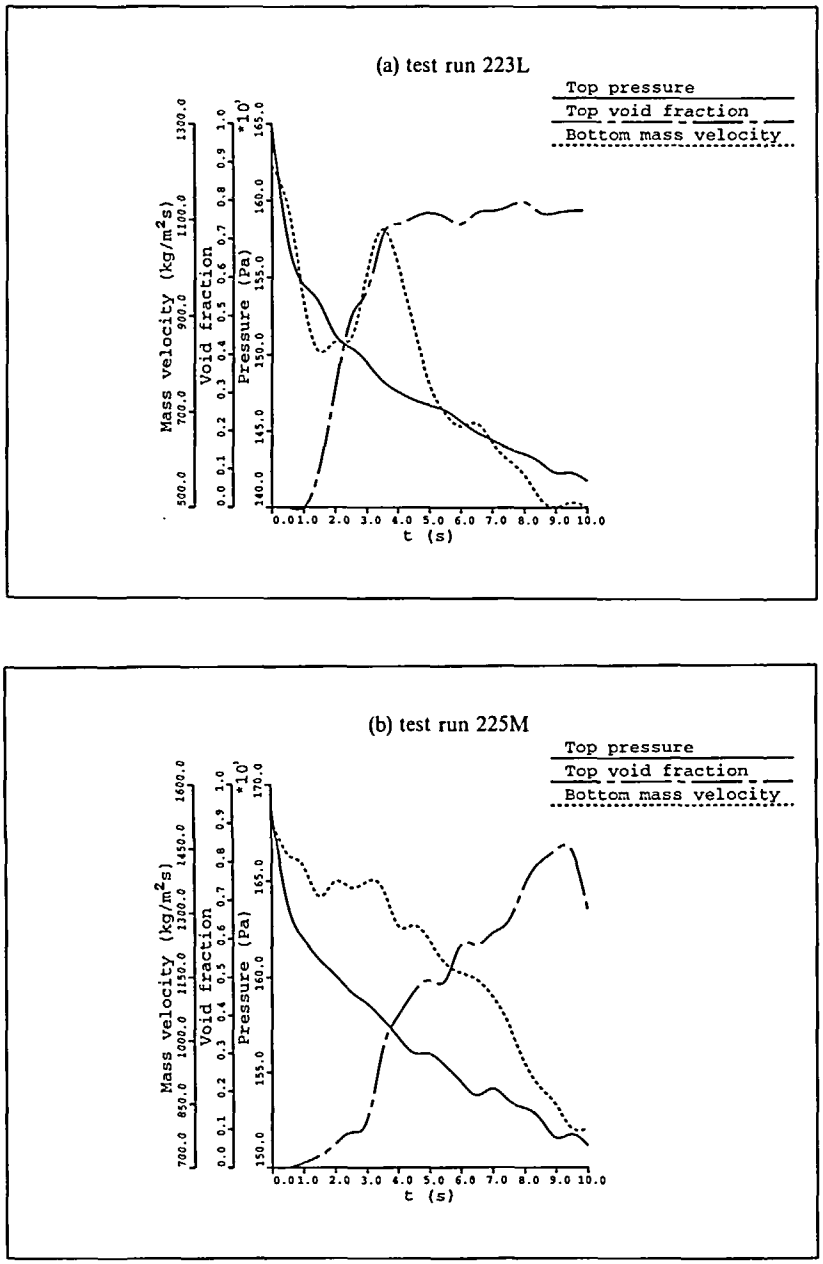

Figure 3 The boundary conditions for the simulation of Ng's experiments

It can be seen that the agreement between the simulated values and the experimental results is good in general except that for runs 225M and 214LA, where the model underestimates the mid-section void fraction by about 10% though it correctly predicts the onset of the local cavitation and the variation of bottom pressure. The reason for this discrepancy is not clear. There are also some oscillations in *Figures 5* and *6*, which might be due to the use of HEM

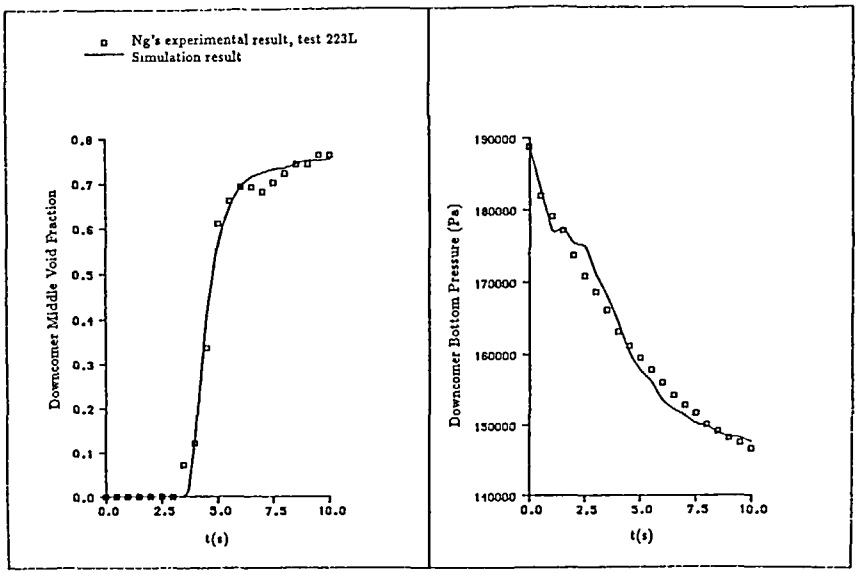

Figure 4 The comparisons of model calculations with Ng's experimental results

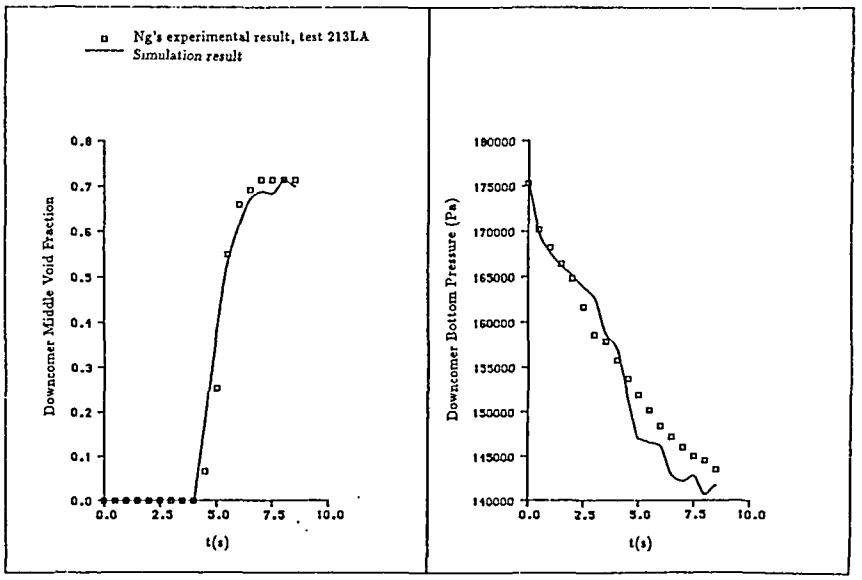

Figure 5 The comparisons of model calculations with Ng's experimental results

while the imposed boundary conditions, being experimental values, might carry considerable non-equilibrium information. Nevertheless, the overall good agreement indicates that the present model is applicable. And the fairly good prediction on the void fraction transient, in particular, on the onset of cavitation at the mid-section may indicate that the model is capable of catching the propagating void front.

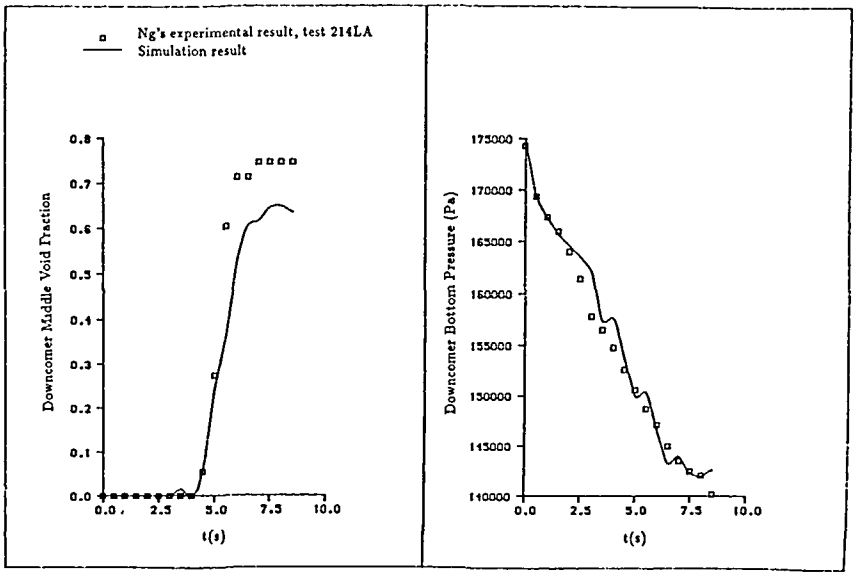

Figure 6 The comparisons of model calculations with Ng's experimental results

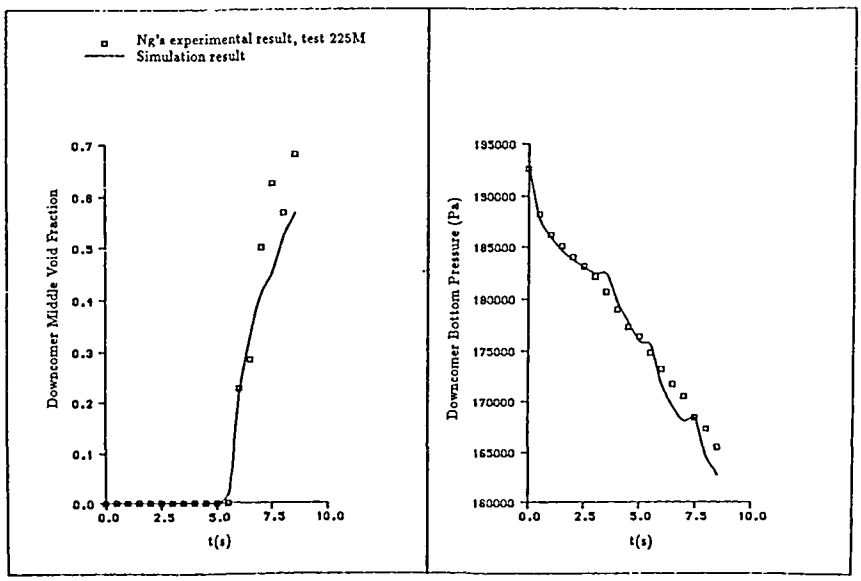

Figure 7 The comparisons of model calculations with Ng's experimental results

Table 1 The run set-ups of Lu's tests

	5LS1	54LS1	54LS3	56LS1
P_{d0} ($\times 10^5$ Pa)	1.16	1.08	1.13	1.14
V_0 (m^3)	0.06	0.05	0.05	0.06
m_{inj} (kg/s)	0.279	0.279	0.279	0.279
M_{b0} (kg/s)	0.60	0.89	1.06	1.07

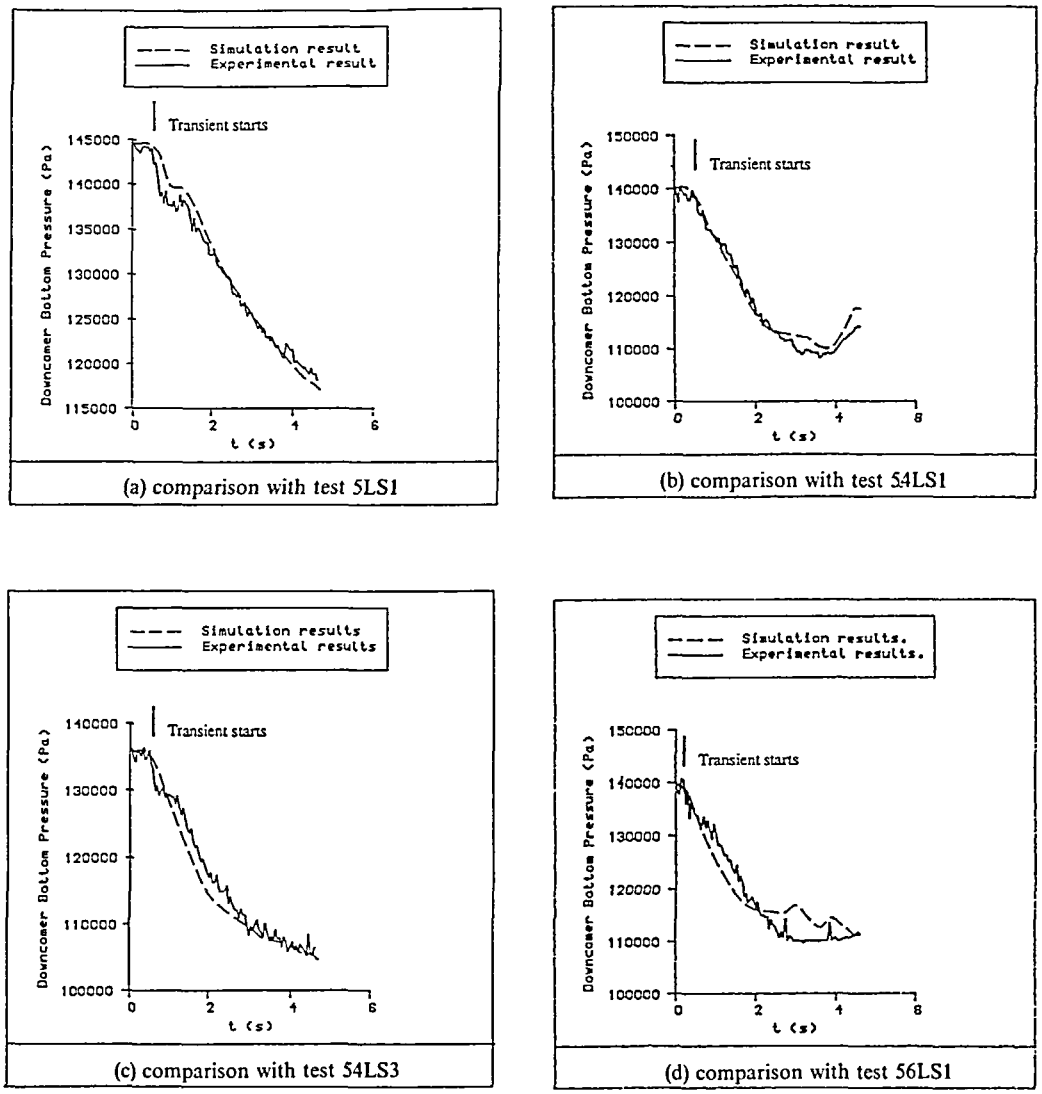

Figure 8 The comparison of simulation results with Lu's experimental data

The comparison of model calculations with Lu's[12] experimental data

The present model was also validated against Lu's[12] experimental results.

A mesh with the same number of nodes as the one described previously and the same optimum *Co* as previously defined were used for the calculations. Similar boundary conditions to those described above were imposed. However, Lu's α_t was estimated by using a semi-empirical model as it was not measured. while P_t and G_b were experimental values. The run set-ups of each test presented here are given in *Table 1.*

Typical results are shown as in *Figure 8.* The void fraction at the mid-section was not measured, hence only the pressure P_b at the downcomer bottom is available for comparison.

The pressure plateau in *Figures 8*(a) and *8*(b) at about 1 sec reflects a considerable pressure recovery in the drum. It can be seen that the agreement between the numerical simulations and the experimental results are generally satisfactory. It is also noteworthy that the flow patterns in the downcomer in Lu's experiments were observed to be like annular flow.

CONCLUDING REMARKS

A simple, transient two-phase flow numerical model was developed based upon the homogeneous equilibrium model (HEM) and the application of split-coefficient matrix method (SCMM). The model was validated against experimental data. It is numerically stable and easy to use. Hence, it may be used by engineers, who need little knowledge about CFDs, for transient two-phase flow system design or analyses.

The present work also demonstrates the potential of SCMM for transient two-phase flow numerical solution. Apart from having the same advantages as the method of characteristics, it is more convenient to code and use. And in principle, it is more accurate than the numerical schemes using stabilising techniques such as artificial damping terms, and staggered mesh and donor-cell techniques. The advantages of SCMM, we believe, will be highlighted when it is applied to more complicated considerations. It should, however, point out that the SCMM can only be applied to well-oposed mathematical systems, i.e. the systems have real eigenvalues.

REFERENCES

1 Wallis, G. B. *One-Dimensional Two-Phase Flow*, McGraw-Hill, New York (1969)
2 Ishii, M. *Thermo-Fluid Dynamic Theory in Two-Phase Flow*, Eyrolles, Paris (1975)
3 Banerjee, E. and Hancox, W. T. On the development of methods for analyzing transient flow boiling, *Int. J. Multiphase Flow*, **4**, 437–460 (1978)
4 Micaelli, J. C. Numerical methods in advanced safety codes, in *Transient Phemomena in Multiphase Flow*, Ed. by N. H. Afgan, 787–798, Hemisphere Publ. Corp. (1988)
5 Jackson, J. F., Liles, D. R., Ransom, V. H. and Ybarrondo, L. J. LWR system safety analyses, in *Nuclear Reactor Safety Heat Transfer*, Ed. by O. C. Jones Jr., Hemisphere Publ. Corp. (1981)
6 Courant, R., Isaacson, E. and Rees, M. On the solution of non-linear hyperbolic differential equations by finite differences, *Comm. on Pure and Applied Maths.*, **5**, 243–255 (1952)
7 Hancox, W. T., Mathers, W. G. and Kawa, D. Analysis of transient flow-boiling, application of the method of characteristics, *A.I.Ch.E. paper 42*, 15th National Heat Transfer Conference, San Francisco (1975)
8 Ng, K. C. *Aspects of Transient Two-Phase Flow*, Ph.D. thesis, University of Strathclyde, Glasgow (1980)
9 Chakravarthy, S. R., Anderson, D. A. and Salas, M. The split-coefficient matrix method for hyperbolic systems of gas dynamic equation, *AIAA paper 80-0268* (1980)
10 Steger, J. L. Coefficient matrices for implicit finite difference solution of the inviscid fluid conservation law equation, *Comput. Methods Appl. Mech. Eng.*, **13**, 175–188 (1978)
11 Steger J. L. and Warming, R. F. Flux vector splitting of the inviscid gas dynamic equations with application to finite difference methods, *J. of Comput. Physics*, **40**, 263–293 (1981)
12 Lu, D. M. *Theoretical and Experimental Investigation of Deaerator System Transient Depressurisation*, Ph.D. thesis, University of Strathclyde, Glasgow (1993)

APPENDIX 1

THE EXPRESSIONS FOR JACOBIAN SUB-MATRICES D^+ AND D^-

The sub-matrices D^+ and D^- of the Jacobian matrix D of (15) are obtained as,

$$D^+ = \begin{bmatrix} x_1 & x_2 & x_3 \\ x_4 & x_5 & x_6 \\ x_7 & x_8 & x_9 \end{bmatrix} \tag{A1}$$

and

$$D^- = \begin{bmatrix} y_1 & y_2 & y_3 \\ y_4 & y_5 & y_6 \\ y_7 & y_8 & y_9 \end{bmatrix} \tag{A2}$$

In (A1) and (A2)

$$x_1 = \frac{\lambda_1^+(1+u/c)+\lambda_2^+(1-u/c)}{2} \tag{A3}$$

$$x_2 = \frac{\lambda_1^+(1+u/c)(1-uC(\rho k)_m)-\lambda_2^+(1-u/c)(1+uC(\rho k)_m)}{2C} - \frac{\lambda_3^+ u}{C^2 e} \tag{A4}$$

$$x_3 = -\frac{\lambda_1^+(1+u/c)+\lambda_2^+(1-u/c)}{2}\rho_{gf}u + \lambda_3^+ \rho_{gf} u \tag{A5}$$

$$x_4 = \frac{C(\lambda_1^+ - \lambda_2^+)}{2} \tag{A6}$$

$$x_5 = \frac{\lambda_1^+(1-uc(\rho k)_m)+\lambda_2^+(1+uc(\rho k)_m)}{2} \tag{A7}$$

$$x_6 = \frac{\lambda_2^+ - \lambda_1^+}{2} C\rho_{gf} u \tag{A8}$$

$$x_7 = \frac{\lambda_1^+ - \lambda_2^+}{2C\rho_{gf} e} \tag{A9}$$

$$x_8 = \frac{\lambda_1^+(1-uC(\rho k)_m)+\lambda_2^+(1+uC(\rho k)_m)-2\lambda_3^+}{2C^2\rho_{gf} e} \tag{A10}$$

$$x_9 = \frac{-\lambda_1^+ u + \lambda_2^+ u}{2Ce} + \lambda_3^+ \tag{A11}$$

and

$$y_1 = \frac{\lambda_1^-(1+u/c)+\lambda_2^-(1-u/c)}{2} \tag{A12}$$

$$y_2 = \frac{\lambda_1^-(1+u/c)(1-uC(\rho k)_m)-\lambda_2^-(1-u/c)(1+uC(\rho k)_m)}{2C} - \frac{\lambda_3^- u}{C^2 e} \tag{A13}$$

$$y_3 = -\frac{\lambda_1^-(1+u/c)+\lambda_2^-(1-u/c)}{2}\rho_{gf}u + \lambda_3^- \rho_{gf} u \tag{A14}$$

$$y_4 = \frac{C(\lambda_1^- - \lambda_2^-)}{2} \tag{A15}$$

$$y_5 = \frac{\lambda_1^-(1-uC(\rho k)_m)+\lambda_2^-(1+uC(\rho k)_m)}{2} \tag{A16}$$

$$y_y = \frac{\lambda_2^- - \lambda_1^-}{2} C\rho_{gf} u \tag{A17}$$

$$y_7=\frac{\lambda_1^- - \lambda_2^-}{2C\rho_{gf}e} \tag{A18}$$

$$y_8=\frac{\lambda_1^-(1-uC(\rho k)_m)+\lambda_2^-(1+uC(\rho k)_m)-2\lambda_3^-}{2C^2\rho_{gf}e} \tag{A19}$$

$$y_9=\frac{-\lambda_1^- u+\lambda_2^- u}{2Ce}+\lambda_3^- \tag{A20}$$